SAILPLANE WINGLET DESIGN THROUGH DIRECT SEARCH OPTIMIZATOIN BASED ON A NON-LINEAR AERODYNAMIC MODEL

Paulo Henriques Iscold Andrade de Oliveira, iscold@ufmg.br
Ricardo Luiz Utsch de Freitas Pinto, utsch@ufmg.br
Luiz Augusto Tavares Vargas, luizatv@superig.com.br
Universidade Federal de Minas Gerais
Av. Antônio Carlos, 6627 – Pampulha – 31270-901- Minas Gerais - Brasil

Abstract. *This paper presents a computational method to assist the design of a sailplane winglet using a direct search optimization procedure. Particullary, the pattern search was used. The aerodynamic model used for this analyses is a non-linear model based on vortex-lattice method, that is able to predict the aerodynamic behavior of lifiting surface beyond to stall. It is also included in this analyses the effects of free wake and the calculation of induced drag through the analyses of a Treftz palne. A study case using the PIK-20B sailplane is presented in order to show the feasiability of this procedure.*

Keywords*: winglet, vortex lattice, optimization*

1. INTRODUCTION

The increased performance of modern aircrafts has established the need for aerodynamic devices that permits performance gains and fuel consumption reduction, and one of the most studded and analyzed device have been the winglets [28]. The interest in winglets is not only for new designs but also for existing aircrafts that can be retrofitted with these devices. Although the continuous interest in the design process of this device, the analysis tools continues needing additional research and improvements.

Being a winglet a device that reduces the wing induced drag adjusting the lifting distribution over the span, the main reference to be understood before its design is the early work of Munk [1]. But the work of Munk is restricted to single dihedral and the design of more complex shapes, like crescent-moon planforms [2, 3], can't be analyzed strictly in this scope, and further work must be used [4, 5, 6].

In these works, the design of a wingtip device, particularly a winglet, is treated as a problem of minimize the wing drag in a particular flight condition. This minimization must take into consideration both: i) the reduction in induced drag due the best lift distribution achieved and ii) the increase in parasite drag due the increase of wetted area. Different aerodynamic procedures are used to calculate the wing induced drag, from the lifting-line theory to high order panel methods [2, 3, 4]. The use of Wessinger Method [7] and some variations of that seem to be a good choice to analyze winglets, with a good compromise between accuracy and computational cost. Methods for induced drag estimation are discussed in many papers, but it is consensus that the Trefftz-plane calculation with plain wake aligned with the free-stream produce the better results [3,5].

Particularly for sailplanes, Maughmer [6] present a detailed discussion about the winglet design process, including important issues about the determination of airfoil, chord distribution, height, twist sweep and toe angle. In addition, Maughmer analyze the problem of winglet design in light of a typical sailplane cross-country flight. In this way is introduced the concept of crossover point, i.e. the airspeed value at which the base aircraft flight polar intersect the polar of the aircraft with winglets. However, Maughmer notices that even introducing aspects of cross-country flight still difficult to determine the optimal design of a winglet, since the weather conditions have a major impact in this optimization.

In this paper, the design of a sailplane winglet is performed using a direct search optimization procedure, in order to determine the geometry that maximizes the sailplane glide ratio in a predefined airspeed. Using the results of this problem is possible to analyze the cross-country performance of the sailplane and then, according to the weather condition, determine the best choice.

A non-linear lifting line procedure, that includes Trefftz-plane induced drag calculations and free-wake, is described, highlighting relevant aspects of its use in this optimization procedure. The direct search adopted is a Pattern Search Method, which is also discussed and detailed. An example of the design of a winglet for a FAI 15m sailplane is presented, showing the performance of the proposed procedure. In this work, only the aerodynamic aspect of the implementation of a winglet was analyzed, other aspects such structural and weight, must be analyzed prior the final decision to use a winglet.

2. PROBLEM DEFINITION

The problem to be solved in this work is the determination of the geometry of a sailplane winglet that maximize the sailplane glide ratio (L/D) at a given flight condition (V). The complete winglet geometry is defined by seven

parameters (Figure 1): i) root chord ; ii) tip chord; iii) root toe-in angle; iv) tip toe-in angle; v) sweep angle; vi) dihedral angle and vii) winglet span.

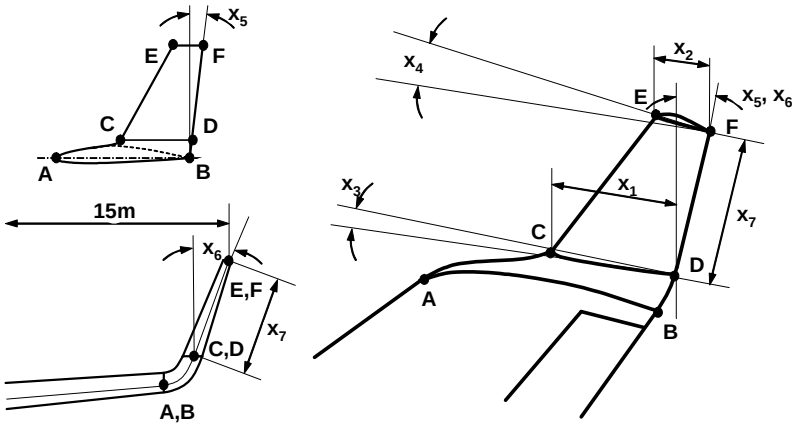

Figure 1 – Winglet geometry definition used in optimization procedure

Must be noticed that in order to agree with FAI 15m and Standard sailplanes rules (*Federation Aeronautique Internationale*) the total wing-span of the sailplane, measured between most out-ward parts of the wing must be at most 15 meters. Thus, if a winglet with dihedral angle greater then 0 degrees is added on a 15 meters wing, must be necessary to reduce the original wing span in order to meet this rule.

Therefore, the optimization problem can be written as:

$$\max_{x} \left. \frac{L}{D} \right|_{V} (x_i) \quad i = 1 \ldots 7 \tag{1}$$

Where the optimization variables are subjected to inequality constraints of the type:

$$x_{i\min} \leq x_i \leq x_{i\max} \tag{2}$$

It is important to note that in each flight condition a new equilibrium configuration (elevator deflection and attack angle) must be calculated. Details about this calculation will be shown in optimization procedure section.

The airfoils used in the winglet will be predefined and not participate of the optimization procedure. In the example presented in following section, the PSU 94-097 airfoil is used for the winglet.

Must be noted that is analyzed only the aerodynamic problem of a winglet design. Aspects such loads, weight increment and flutter airspeed reduction must be investigated separately.

3. AERODNAMIC MODEL

The proposed procedure to calculate the aerodynamic characteristics of the wing, with or without the winglet, is a variation of Wessinger Method [7], that uses the bidimensional characteristics of the airfoils that composes the wing in order to take into consideration the viscous drag of the wing and to predict the wing behavior beyond the stall. Additionally, this procedure has a free-wake methodology and the induced drag is calculated in a Trefftz-plane, in order to be predicted more precisely. The following will describe the construction of this procedure.

Originally, Vortex-Lattice method is based on the solution of the Laplace equation through the distribution of singularities (horseshoe vortex) along the span as well as in the camber line of the airfoil, which responds to the condition of impermeability (flow cannot pass throughout a non-porous surface). However, in the proposed method, since bi-dimensional information on the aerodynamic airfoil would be used, the distribution along the chord becomes unnecessary. This method is also known as Wessinger [7], or modern lifting line [8]. The distribution of bounded vortex is at every ¼ of chord, and the control points are at ¾ of chord, satisfying the Kutta's condition in the trailing edge.

Instead of using the classic flat horseshoe vortex, in this procedure the vortex is composed by discrete vortex segments (Figure 2) which, follows the surface until the trailing edge and than align to the free stream [9]. In this way is possible to include a free wake procedure.

The solution of a vortex-lattice model is based on a development of the Bio-Savart theorem [10]. The speed in point P induced by a straight vortex line segment that goes from point A to point B, can be calculated through the equation (3)

$$\vec{V} = \frac{\Gamma}{4\pi} \frac{\vec{r}_1 \times \vec{r}_2}{\left|\vec{r}_1 \times \vec{r}_2\right|^2} \vec{r}_0 \cdot \left(\frac{\vec{r}_1}{\left|\vec{r}_1\right|} - \frac{\vec{r}_2}{\left|\vec{r}_2\right|} \right) \tag{3}$$

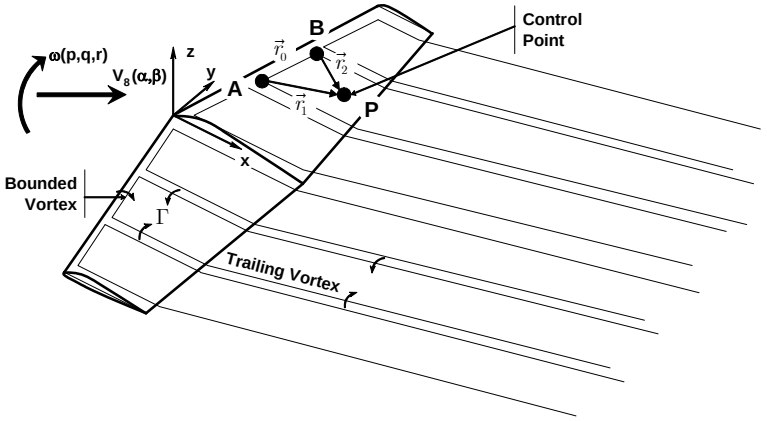

Figure 2 – Vortex Lattice Arrangement adopted in the proposed aerodynamic procedure.

Where $\vec{v}$ denotes the speed induced by a vortex segment, Γ denotes the intensity of the vortex and $\vec{r}_0$, $\vec{r}_1$ and $\vec{r}_2$ are the distances between points A and B, A and P and B and P, respectively.

The solution of the potential flow problem will be the determination of the intensities Γ of each horseshoe vortex through a system of linear equations as shown in equation (4), with the boundary condition being the condition of body impermeability.

$$\begin{bmatrix} w_{11} & w_{12} & \cdots & w_{1n} \\ w_{21} & w_{22} & \cdots & w_{2n} \\ \vdots & \vdots & \vdots & \vdots \\ w_{m1} & w_{m2} & \cdots & w_{mn} \end{bmatrix} \times \begin{Bmatrix} \Gamma_1 \\ \Gamma_2 \\ \vdots \\ \Gamma_n \end{Bmatrix} = \begin{Bmatrix} B_1 \\ B_2 \\ \vdots \\ B_n \end{Bmatrix} \tag{4}$$

Where w_{mn} denotes the geometric influence on normal induced speed on the panel m by the horseshoe vortex n, Γ_n denotes the intensity of the horseshoe vortex n and B_n denotes the speed of normal free flow at the panel surface in the control point n, including the components due to angular velocities (rolling, pitch and yaw).

Once the intensity of each horseshoe vortex is determined, the aerodynamic forces can be calculated according to the Kutta-Joukowsky theorem as show in equation (5) [10] resulting in the distribution of force, in each panel, as shown in Figure 4.

$$\vec{F} = \rho \vec{V} \times \vec{\Gamma} \tag{5}$$

Where $\vec{F}$ denotes the resulting force at ¼ of the chord, ρ the fluid density, $\vec{V}$ the resulting vector for the speed at ¼ of chord and $\vec{\Gamma}$ the bounded vortex intensity.

Since the distribution of horseshoe vortex occurs only along the span, with only one control point along the chord disregarding the line of camber of the airfoil, the results obtained with the traditional method refer to a wing that uses a symmetric aerodynamic profile, which, according to the linear theory is equivalent to a flat plate, with a lift slope constant equal to 2π and the null lift angle constant and equal to zero.

In order correct the three-dimensional results of flow obtained with the flat plate as a function of aerodynamic characteristics of the real airfoil, an iterative process similar on the methods presented by [11, 13, 14 and 15] will be used.

The proposed iterative process uses the bidimensional aerodynamics information of the airfoils that compose the wing in order to adjust the relation between the attack angles and lift coefficients obtained through the vortex-lattice method. This is done using an incremental value (δ) to each local effective attack angle calculated by the vortex-lattice method. This value is iteratively determined in order to cancel the difference (ΔC_L) of lifting coefficient calculated by vortex-lattice method and lifting coefficient obtained by bidimensional aerodynamic information of the airfoil. More detailed, this procedure can be explained in the follow algorithm.

1. *Initial values of δ and ΔC_L are assumed for each section of the wing.*
2. *The aerodynamic characteristics of the wing are calculated using the traditional vortex-lattice algorithm*
3. *The effective attack angles for each section ($\alpha_{e\_\sec}$) are calculated using the local lift value obtained in step (2) using the equation (4):*

$$\alpha_{e\_\sec} = \frac{C_{L\sec}}{2\pi} - \delta \tag{6}$$

4. *The value of* $\Delta C_L = C_{Lvisc} - C_{L\sec}$*, is calculated, where* $C_{L\sec}$ *is the value obtained with the conventional vortex-lattice method, and* C_{Lvisc} *is the value obtained using the information of the airfoil and effective attack angle for each section of the span (bi-dimensional polar curves).*
5. *The new value of* δ *is calculated using equation (7) and the new angle of attack of witch sections became the initial angle of attack plus the new value of* δ*, as show in equation (8) .*

$$\delta = \delta + \frac{\Delta C_L}{2\pi} \tag{7}$$

$$\alpha_{e\_\sec} = \alpha_{initial} + \delta \tag{8}$$

6. *Return to (2), where* $\alpha_{e\_\sec}$ *is the new value for the attack angle of each section to be used for the calculation with the traditional method. This process is repeated until* $C_{L\sec}$ *converges.*

When the effective attack angle for each station and the airfoil polar is known, beyond getting the lift coefficient, it is also possible to obtain the parasite drag and aerodynamic moment coefficients for each wing section.

Mukherjee, Gopalarathnam and Kim [11] tested the algorithm only in individual wings in simple flight conditions (without angular velocities) and observes several numerical instabilities when the slope of the bidimensional lift curve became negative. This behavior, in accordance to Sears [12] has been noticed by Von Kármán as a typical behavior of Prandtl's lifting line equation when lifting line have negative gradient. These nonunique solutions include both symmetrical and antisymmetric lift distributions even when the geometry and onset flow are both symmetric. In order to use the proposed algorithm in a complete aircraft with multiple wings and tails with complex geometries subject to non-symmetrical flight conditions, it was necessary to use a damping and dissipation coefficients, which are not included in the original algorithm, bringing more stability to the numeric method. Thus, the equation (5) was transformed into the form shown in equations (9) and (10).

$$\delta_i = \delta_i + \frac{1}{K+1}\frac{\Delta C_L}{2\pi} \tag{9}$$

$$\delta_i = \frac{\left(\delta_i + \Pi\dfrac{\left(\delta_{i-1} + \delta_{i+1}\right)}{2}\right)}{1+\Pi} \tag{10}$$

Where i denotes the section throughout the span, K is the damping factor and Π is the dissipation factor.

Because the difficulties associated with the calculation of the induced drag present in a lifting surface, there is many ways to estimate it. However, Eppler [4] and Smith and Kroo [3] suggest that the best way to calculate it is computing the pressure and momentum integral over a control volume surrounding the wing (Figure 3).

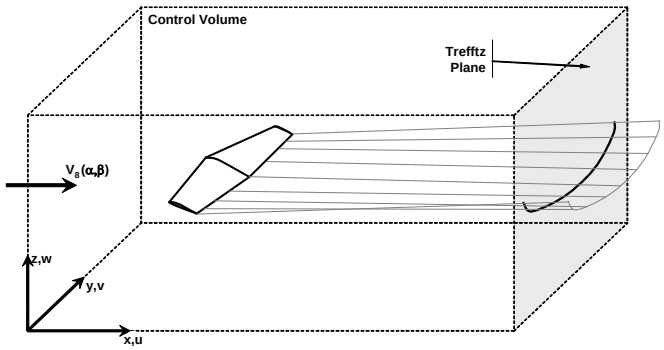

Figure 3 – Sketch of Trefftz Plane arrangement

$$D_{IND} = \frac{1}{2}\rho\int_{-\infty}^{\infty}\int_{-\infty}^{\infty}\left(v^2 + w^2\right)dydz \tag{11}$$

Taking into consideration that the control volume extends to infinity and that the trailing vorticity is confined to a thin wake sheet, where the horizontal component is negligible, this integral reduces to a contour integral along the intersection of the trailing vortex wake with the control volume exit-plane [3]. This method is called Trefftz Plane integral and relates the induced drag to the jump in potential across the wake, and the normal flow velocity through the wake.

$$D_{IND} = \frac{1}{2}\rho \int_{-b/2}^{b/2} \Delta\phi \cdot W_{tp}\, ds \tag{12}$$

Where $\Delta\phi$ denotes the difference of potential between the top and the bottom side of the wake, and W_{tp} is the normal flow velocity thought the wake.

As in the method of horseshoe vortex distribution, the difference in potential in the wake is the circulation ($\Delta\phi = \Gamma$),the induced drag could be conveniently calculated through the equation.(13).

$$D_{IND} = \frac{1}{2}\rho \sum_{i=1}^{n} \Gamma_i W_{tpi} s_i \tag{13}$$

Where D_{IND} denotes the induced drag, ρ denotes the density of the fluid, Γ the intensity of the horseshoe vortex, W_{tp} the normal induced velocity through the wake and s the width of the horseshoe vortex.

Although this formulation is also valid for any wake form, even for the rolled-up vortex sheet [16], Eppler [4] and Smith and Kroo [3] notice that the remain small discrepancies in the modeling of vortices rolling up may produce numerical errors of a level similar to the induced drag increments themselves. Thus, as suggested in [5], the best approach is to use a rigid plane wake parallel to the free-stream direction accepting the errors in induced velocities. Smith and Kroo [3] notice that although the straight wake is not force-free, it is drag-free, since the vorticity is parallel to the free-stream. Therefore, this approach is expected to agree (errors less than 2%) with the drag that would be determined from perfect surface pressure integration.

Even though the wake rolling up would not be used in the estimation of induced drag, its calculation is important in order to modeling complete geometries, including wing and tail. Furthermore, the alignment of the horseshoe vortex with the free wake is important for the calculation of fixed wing aircrafts in severe flight conditions (angular rates) in which the wake passes very close to other lift surface [17].

In order to solve this problem, a free wake model can be added to the Vortex-Lattice model. This is a non linear and transient iterative process which demands long processing time, since the wake is discretized in distinct elements and the horseshoe vortex trajectory is calculated.

The algorithm used for the calculation of the free wake is based on the ideas proposed by Katz and Maskew [17] and can be described as following (Figure 4):

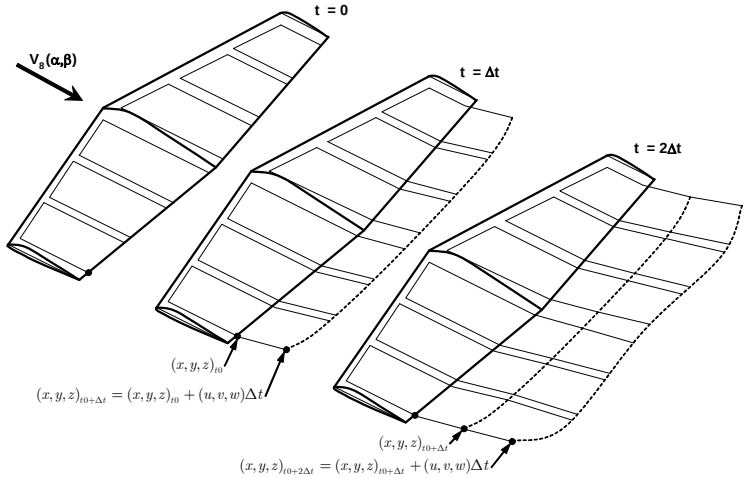

Figure 4 – Free wake integration schema

1. *Assume a initial geometry for the horseshoe vortex where the trailing vortex extend on the body surface from the bonded vortex (¼ of chord) to the trailing edge only (instant t = 0 in Figure 4).*
2. *The vortex-lattice method is used in order to calculate the intensity of the vortex and the velocity in the control points of the wake.*

3. *With the velocities in the control points, the trajectory of a fluid particle located on these points is calculated (stream lines) using a numerical integrator, as shown in equations (14) and (15).*

$$(x, y, z)_{t0+\Delta t} = (x, y, z)_{t0} + (\Delta x, \Delta y, \Delta z) \quad (14)$$

Where:

$$(\Delta x, \Delta y, \Delta z) = (u, v, w)\Delta t \quad (15)$$

4. *The trailing vortex is then extended over the calculated fluid particle trajectory (stream line).*
5. *Return to step (2), until the convergence of criteria adopted or a pre-established number of iterations is obtained.*

It is important to noticed that this is an elliptic problem. In other words, it is necessary to re-calculate the entire wake at each iteration, since the most distant vortex segment of the wing modifies the beginning of development of the wake, closest to the wing.

It is also important to highlight that in step (2), the equations (14) and (15) refer to a first order integrator (Euler). It is advisable to use a numeric integrator of superior order, such as the Runge-Kutta of second or fourth order, which improves the precision of results.

This procedure was exhaustively tested and compared with experimental results by Vargas [18]. Results have shown very accurate in relation to experimental results, especially for the calculation of wing and tail configurations. In non symmetrical conditions the procedure proof to be very adequate to predict aerodynamic derivatives to be used in dynamic simulations. Regarding to stall and post-stall prediction, the adoption of damping and dissipation coefficients has shown adequate in order to assure unique solutions even in negative gradient regions of airfoil lift curve.

The computational time of typical geometries (including wing, winglet, horizontal and vertical tail) in modern personal computers (Pentium IV, Windows XP, 1Gb RAM) is about 5 seconds, including free-wake and drag prediction through Trefftz Plane.

5. OPTIMIZATION PROCEDURE

Taking into consideration the complexity of this problem, especially the aerodynamic model, is expected that common optimization procedures that demand the derivative information will not present desirable performance. Therefore, a direct search method, without derivatives, was chosen, particularly, the Constraint Pattern Search Method [19, 20, 21, 22].

This method is useful to problems where [20, 21]:

- Function is either non-differentiable or the derivative information proves to be unreliable;
- Function is computed to low accuracy
- Function is highly nonlinear
- Only rank (order) information is available

In this work, the high nonlinearity and the difficult (high computational cost) to compute the derivative information of the function justify the use of a Pattern Search Method.

The basic idea behind this method [20, 21] is the exploration of samples in the search space in a fixed direction collection (pattern) around the current point (Figure 5). The algorithm defines a mesh, consisting of points derived from original point (pattern center) plus the pattern multiplied by a scalar, and calculates function values of these points and tries to find the point of minimum (or maximum) value. If it finds a new minimum, then it changes the pattern center and iterates using a double mesh size (scalar multiplier). Otherwise, if all the values on pattern fails to produce a decrease, the mesh size (scalar multiplier value) is reduced to half and the pattern is applied in the same pattern center. This procedure continues until that a convergence criterion is reached. In this work, this criterion was formed by five values i) Minimum mesh size; ii) Maximum number of iterations; iii) Maximum functions evaluations; iv) Optimization variable tolerance and v) Function tolerance.

Therefore, in accordance with previous sections, the optimization problem to be solved by Pattern Search Method was:

$$\min J(x_i) \quad i = 1 \ldots 7 \quad (16)$$

Subjected to

$$x_{i\min} \le x_i \le x_{i\max} \quad i = 1 \ldots 7$$

Where:

$$J(x_i) = \frac{L}{D + D_0} \quad i = 1 \ldots 7 \quad (17)$$

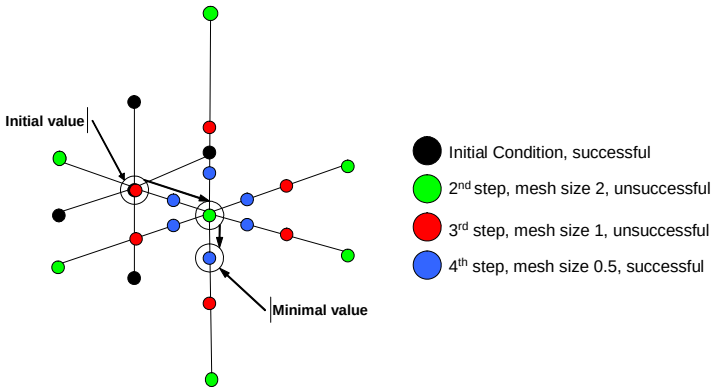

Figure 5 – Example of four iteration of Pattern Search Algorithm in 3-dimensional space.

Where L and D denotes, respectively, the total lifting force and drag force calculated by the proposed aerodynamic procedure, which is relative to wing and tail. D_0 denotes the drag force generated by other aircraft components, such fuselage, landing gear, etc, which is calculated by conventional drag build-up methods [24]. It is assumed that only wing and tail produce lift.

Additionally, as cited before, it is necessary to determine the equilibrium condition (pitch moment and vertical force) for each configuration analyzed by Pattern Search Method. This is solved using an accessory optimization problem of the following form:

For each geometry ($x_i, i = 1 \ldots 7$) analyzed by the Pattern Search Method:

$$\min G(\alpha, \delta) \tag{18}$$

Where:

$$G(\alpha, \delta) = \left[M(\alpha, \delta) + M_0 \right]^2 + \left[L(\alpha, \delta) + W \right]^2 \tag{19}$$

Where L and M denotes, respectively, the lift force and the pitch moment of wing and tail calculated by the aerodynamic model proposed, M_0 is the pitch moment of other aircraft components (fuselage, etc) and W denotes the airplane weight. α and δ denotes, respectively, the airplane attack angle and elevator deflection. The elevator deflection effect is included in the proposed aerodynamic model through the modification of the bidimensional aerodynamic (polar) characteristics of the airfoils that compose the horizontal tail. This modification is done using the linear derivative of lift, drag and pitch moment, summed with the original airfoil polar.

This accessory problem, for each geometry analyzed by the Pattern Search Method, is solved using a standard gradient method.

6. CASE STUDY

In order to demonstrate the results obtained with this procedure, in this section will be shown the analyses of the winglet designed for a PIK-20B sailplane. Although the PIK-20B is not a modern sailplane, it is used in this example because details of its dimensions [25, 26, 27] and airfoils are available in literature [23]. Figure 6 shows the main dimensions and airfoils of this sailplane.

PIK-20B is a FAI 15m sailplane; therefore a winglet design for it must keep the wingspan limited to 15m. In this way, if a winglet is optimized with a dihedral angle greater than 0, it will be calculated a wing-span reduction, in original wing, in order to not violate this restriction.

The proposed optimization procedure was used to design a winglet for this sailplane assuming that its cruising speed is 120km/h with a wingload of 312N/m^2. Figure 7 presents the final geometry obtained for this winglet, and Table 1 details the values of each optimization variable, and denoted in Figure 1.

Table 1 – Final Geometry values for PIK-20B winglet optimized at 120km/h

X_1	0.1413 m	X_5	-0.1394 °
X_2	0.0549 m	X_6	-0.0938 °
X_3	0.3545 °	X_7	0.5 m
X_4	1.5707 °		

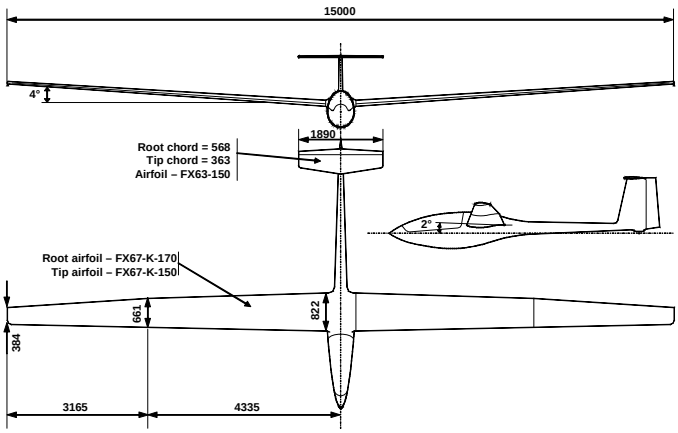

Figure 6 – PIK-20B three views with main dimensions and characteristics used in the aerodynamic model

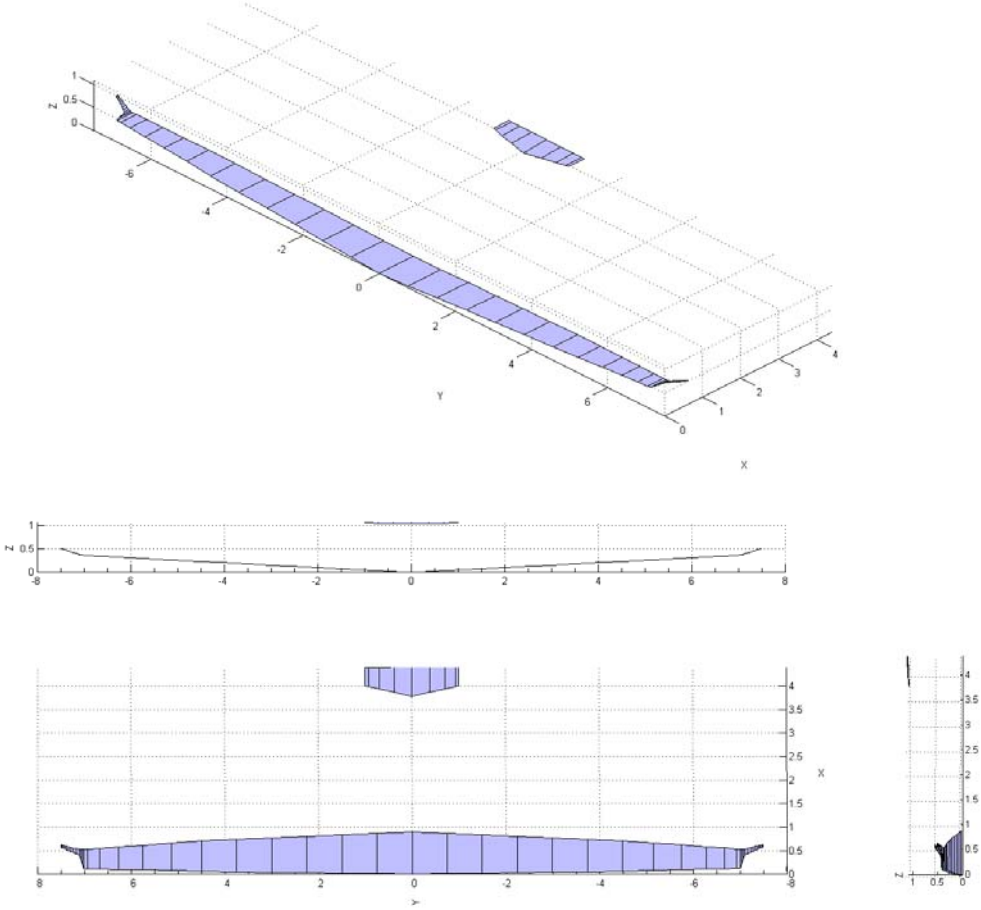

Figure 7 – Final geometry obtained for PIK-20B winglet optimized at 120km/h

In order to analyze the advantage of this winglet to sailplane performance, two comparisons were made. The first one is the increase in maximum glide ratio versus sailplane airspeed, as can see in Figure 8. Can be noted that regarding the fact of this winglet was optimized at 120km/h (2.3% increases in glide ratio), the maximum increase in glide ratio occurs near 160km/h (2.75% increases in glide ratio). For the whole sailplane airspeed envelope, is noted a increase in glide ratio greater than 1%, which in high speeds can means more than 1 point in glide ratio.

The second comparison were made regarding MacCready cruising speed versus expected climb speed in thermals, as can be see in Figure 9. In this case the gain due the winglet is almost 1% for climb speeds from 0.5m/sto 5m/s which are representative in most cases of cross country flights.

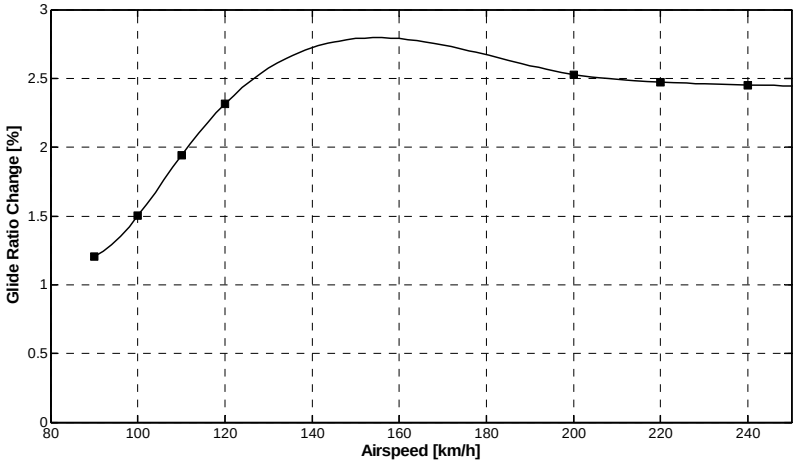

Figure 8 – Glide ratio change due winglet for PIK-20B (wingload = 312N/m^2)

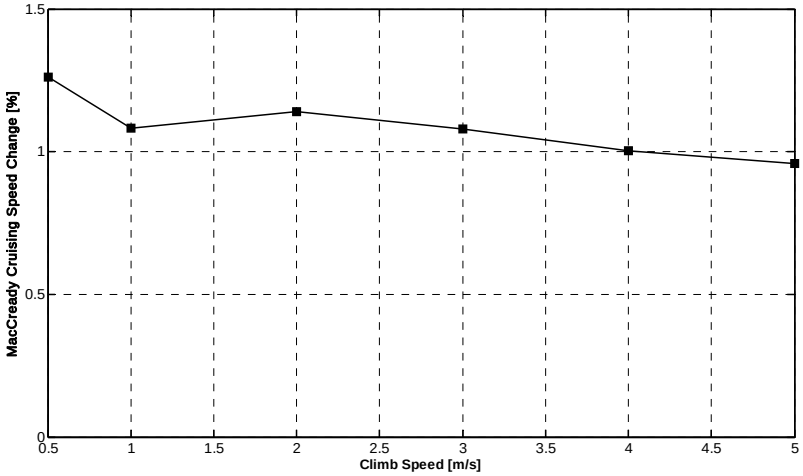

Figure 9 – MacCready Cruising Speed change due winglet for PIK-20B (wingload = 312N/m^2)

5. CONCLUSIONS

This paper presents a computational method for the design of a sailplane winglet using a direct search optimization procedure and a non-linear aerodynamic model. The method is applied to the design of a 15 meters sailplane winglet for a specific airspeed (120km/h) and wingload (312N/m^2). The results show that the proposed procedure can suggest a winglet that increases the sailplane performance. Particularly, the gain in glide ratio reaches 2.7% at 160km/h and for the whole airspeed envelop sustain more then 1%. The gain in MacCready cruising speed is near 1% for climb speeds from 0.5m/s to 5m/s. These results suggest that the procedure is effective in order to help the design of a winglet.

4. REFERENCES

[1] M. M. Munk, The Minimum Induced Drag of Aerofoils, NACA Report 121, (1921).
[2] C. P. VanDam, Induced-Drag Characteristics of Crescent-Moon-Shaped Wings, Journal of Aircraft, (1987), 115-119.
[3] S.C. Smith, I.M. Kroo, Computation of induced drag for elliptical and crescent-shape wings, J. Aircarft 30 (4) (1993) 446-452.
[4] R. Eppler, Induced drag and winglets, Aerospace Science and Technology 1 (1997) 3-15.

[5] A. Büscher, R. Radespiel, T. Streit, Modelling ad design of wing tip devices at various flight conditions using a databased aerodynamic prediction tool, Aerospace Science and Technology 10 (2006) 668-678.
[6] M. Maughmer, The Design of Winglets for High-Performance Sailplanes, AIAA Paper 2001-2406, (2001).
[7] J. Weissinger, The Lift Distribution of Swept-back Wings, NACA Technical Memorandum nº 1120, (1947).
[8] W.F. Phillips; D. O. Snyder, Modern Adaptation of Prandltl´s Liftinf-Line Theory, Journal of Aircraft, vol.37, (4) ,(2000).
[9] L.R. Miranda, R. D. Elliott, W. M. Baker, A Generalized Vortex Lattice Method for Subsonic and Supersonic Flow Applications, NASA CR 2865, (1977).
[10] L. Katz, A. Plotkin, Low- Speed Aerodynamics: From wing Theory to Panel Methods, McGraw-Hill Inc, (1991).
[11] R. Mukherjee, A. Gopalarathnam, S. Kim, An Iterative Decambering Approach for Post-Stall Prediction of Wing Characteristics from Known Section Data, 41st Aerospace Sciences Meeting and Exhibit, Reno, Nevada, (2003).
[12] W. R. Sears, Some Recent Developments in Airfoil Theory, Journal of The Aeronautical Sciences, Vol. 23, (1956), 490–499.
[13] S.T. Piszkin, E. S. Levinsky, Nonlinear lifting line theory for predicting stalling instabilities on wings of moderate aspect ratio -Technical Report, General Dynamics Convair Report CASD-NSC-76-001, (1976).
[14] J. B. Tseng, C. E. Lan, Calculation of aerodynamic characteristics of airplane configurations at high angles of attack, NASA CR 4182, (1988).
[15] K. Jacob, Computation of the flow around wings with rear separation, Journal of Aircraft, Vol. 21, (1984), 97-98.
[16] H. Schlichting, E. Truchenbrodt,H. J. Ramm, Aedorynamics of the Airplane, McGraw-Hill, USA, (1979).
[17] J. Katz, B. Maskew, Unsteady Low-Speed Aerodynamic Model for Complete Aircraft Configurations, Journal of Aircraft, vol.25, (4) , (1987).
[18] L. A. T. Vargas, Desenvolvimento e implementação de um procedimento numérico para cálculo de conjuntos asa-empenagens de geometria complexa em regime de vôo subsônico, Máster Thesis, Programa de Pós Graduação em Engenharia Mecânica – UFMG, Brazil, (2006).
[19] V. Torczon, On the convergence of Pattern Search Algorithms, SIAM Journal on Optimization, Vol. 7, (1), (1997), 1-25.
[20] R. M. Lewis and V. Torczon, Pattern Search Algorithms for Bound Constrained Minimization, SIAM Journal on Optimization, Vol. 9, (4), (1999), 1082-1099
[21] R. M. Lewis and V. Torczon, Pattern Search Methods for Linearly Constrained Minimization, SIAM Journal on Optimization, Vol. 10, (3), (2000) 917-941
[22] C. Audet and J.E. Dennis Jr., Analysis of Generalized Pattern Searches, SIAM Journal on Optimization, Vol. 13, (3), (2003), 889-903.
[23] A. Weise, Stuttgarter Profilkatalog I, Institut für aerodynamik und gasdynamik der technischen hochschule Stuttgart; (1972).
[24] S. F. Hoerner, Fluid-Dynamic Drag, published by author, (1965).
[25] R. H. Johnson, A Further PIK-20B Flight Test Evaluation - Part I, Soaring & Motorgliding, Soaring Society of America, Volume 42, (7), (1978).
[26] R. H. Johnson, A Further PIK-20B Flight Test Evaluation - Part II, Soaring & Motorgliding, Soaring Society of America, Volume 42, (8), (1978).
[27] P. Iscold, R. L. U. F. Pinto, Um Procedimento Alternativo para Cálculo Aerodinâmico de Aeronaves Leves Subsônicas, Congresso SAE Brasil, (1999).
[28] Whitcomb, R. T., A Design Approach and Selected Wind-Tunnel Results at High Subsonic Speeds for Wing-tip Mounted Winglets, NASA Thecnical Note TN-D-8260, (1976).

5. RESPONSIBILITY NOTICE

The author(s) is (are) the only responsible for the printed material included in this paper.